

# IMPLICIT-EXPLICIT TRUST REGION METHOD FOR COMPUTING SECOND-ORDER STATIONARY POINTS OF A CLASS OF LANDAU MODELS

CHENGLONG BAO\*, KAI DENG†, KAI JIANG†, AND JUAN ZHANG†

**Abstract.** We propose an implicit-explicit trust region method for computing second-order stationary points of a class of Landau-type free energy functionals, which correspond to physically (meta-)stable phases. The proposed method is demonstrated through the Landau-Brazovskii (LB) model in this work, while broader applicability to more Landau models of the similar type is straightforwardly extended. The LB energy functional is discretized via the Fourier pseudospectral method, which yields a finite-dimensional nonconvex optimization problem. By exploiting the Hessian structure—specifically, that the interaction potential is diagonal in reciprocal space whereas the bulk energy is diagonal in physical space—we design an adaptive implicit-explicit solver for the trust region subproblem. This solver utilizes the fast Fourier transform to perform efficient matrix-vector products, significantly reducing computational complexity while ensuring provable convergence to the global minimizer of the subproblem. In contrast to existing algorithms that target first-order stationary points, our proposed method can converge to a second-order stationary state, corresponding to a local minimum with theoretical convergence guarantees. Numerical experiments on the LB model demonstrate that the proposed approach efficiently escapes saddle points and significantly outperforms existing first-order schemes. Furthermore, we successfully identify the stable region of the FDDD phase, a structure previously unreported in the LB phase diagram.

**2020 MSC.** 65N22, 65K10, 90C26.

**1. Introduction.** Landau theory constitutes a foundational framework for describing phases and phase transitions across a wide range of physical systems [21, 22]. In this paper, we consider a class of Landau-type energy functionals that contain two components, an interaction potential and a bulk energy term,

$$(1.1) \quad E(\psi(\mathbf{x})) = G(\psi(\mathbf{x})) + F(\psi(\mathbf{x})),$$

where  $\psi(\mathbf{x})$  is the order parameter. In this formulation, the interaction potential  $G(\psi)$  typically involves differential or non-local operators that describe spatial correlations and pattern selection, while the bulk energy term  $F(\psi)$  is a nonlinear potential driving phase transitions. This unified framework encompasses a wide variety of physical models, such as the Ginzburg-Landau model, the Ohta-Kawasaki model, the Swift-Hohenberg model, the LB model, and multi-length-scale models [17, 25, 39, 31, 35]. One of the most important problems in investigating these models is computing both stable and metastable states accurately and efficiently [14, 24], which is crucial for constructing phase diagrams and guiding the design of ordered materials in modulated systems.

In the field of scientific computation, a standard approach is to discretize the energy functional (1.1), thereby transforming the infinite-dimensional variational problem into an  $n$ -dimensional optimization problem. By minimizing the resulting discretized function  $E$ , we can obtain the stationary points of the system. We define first- and second-order stationary points (SP-I and SP-II) as follows.

---

\*Yau Mathematical Sciences Center, Tsinghua University, Beijing, 100084, China (clbao@mail.tsinghua.edu.cn).

†School of Mathematics and Computational Science, Hunan Key Laboratory for Computation and Simulation in Science and Engineering, Key Laboratory of Intelligent Computing and Information Processing of Ministry of Education, Xiangtan University, Xiangtan, Hunan, 411105, China (kdeng1533@smail.xtu.edu.cn, kaijiang@xtu.edu.cn, zhangjuan@xtu.edu.cn).

DEFINITION 1.1. For a twice differentiable function  $E : \mathbb{R}^n \rightarrow \mathbb{R}$ , a point  $\mathbf{v} \in \mathbb{R}^n$  is called a first-order stationary point (SP-I) of  $E$  if it satisfies  $\nabla E(\mathbf{v}) = 0$ . Moreover, if  $\mathbf{v}$  is SP-I and satisfies  $\nabla^2 E(\mathbf{v}) \succeq 0$ , then  $\mathbf{v}$  is called a second-order stationary point (SP-II) of  $E$ .

SP-Is encompass global minima, local minima, and saddle points (SDPs), corresponding to stable, metastable and transition states, respectively. SP-IIs form a subset of SP-Is and represent physically stable and metastable states. The identification of SP-IIs enables accurate determination of equilibrium states. We define SP-IIs using positive semi-definite Hessians, rather than strictly positive definite ones, to accommodate degenerate stationary states with zero eigenvalues in their Hessian matrices. Such degeneracy arises fundamentally from continuous symmetries, most notably translational invariance in ordered phases including periodic crystals and quasicrystals [4, 14, 13].

The current algorithms that aim to compute stationary states for such Landau models can be broadly classified into three categories. The first category is to solve the steady nonlinear Euler–Lagrange equations of (1.1). The second category focuses on solving the nonlinear gradient flow equation. Approaches include explicit-implicit schemes [36, 11, 33], the scalar auxiliary variable [32], the invariant energy quadrature scheme [38], and exponential time differencing methods [16]. The third category is from the optimization viewpoint. These approaches directly find the stationary states via solving a finite-dimensional or infinite-dimensional nonconvex optimization problem, such as gradient descent [28, 34], proximal gradient, and the Bregman proximal gradient approaches [4, 3, 18]. However, these approaches typically only consider convergence to SP-Is and theoretically cannot guarantee convergence to SP-IIs.

To address this limitation, this work develops an algorithm that can provably converge to SP-IIs with theoretical guarantees by combining recent advances in optimization. In particular, recent theories suggest that SP-IIs in nonconvex problems can be reached either through controlled perturbations or by exploiting curvature information. Stochastic gradient descent and its adaptive forms escape from saddle points and converge to SP-IIs by introducing noise during the iteration [20, 23]. Trust region (TR) methods [15, 29], and the variants of Newton’s method [27, 30, 1] can also ensure convergence to SP-IIs by utilizing the Hessian information.

To validate the effectiveness of the proposed algorithm, we employ the LB model as a primary benchmark. This model is a representative example that describes systems exhibiting spatially modulated phases at finite wavenumbers, such as block copolymers, liquid crystals, microemulsions, and magnetic materials [7, 35, 8]. It effectively captures a broad spectrum of ordered phases, including lamellar, hexagonal, body-centered cubic spheres, face-centered cubic spheres, double gyroid, A15, and  $\sigma$  phase [26]. The energy functional of the LB model is

$$(1.2) \quad E(\psi(\mathbf{x})) = \frac{1}{|\Omega|} \int_{\Omega} \underbrace{\frac{1}{2} [(\Delta + 1)\psi(\mathbf{x})]^2}_{G(\psi(\mathbf{x}))} + \underbrace{\left( \frac{\tau}{2!} \psi(\mathbf{x})^2 - \frac{\gamma}{3!} \psi(\mathbf{x})^3 + \frac{1}{4!} \psi(\mathbf{x})^4 \right)}_{F(\psi(\mathbf{x}))} d\mathbf{x}.$$

Here,  $\Omega$  is a bounded domain with volume  $|\Omega|$ ;  $\tau$  is the dimensionless reduced temperature, and  $\gamma$  is the phenomenological coefficient. The order parameter  $\psi(\mathbf{x})$  satisfies the mass conservation constraint  $\frac{1}{|\Omega|} \int_{\Omega} \psi(\mathbf{x}) d\mathbf{x} = 0$ .

The main contributions of this paper include

- We propose an implicit-explicit trust region (IMEX-TR) method for a class of Landau-type models, which converges to SP-IIs with theoretical guarantee.

- By exploiting the diagonal structure of the Hessian—diagonal in reciprocal space for the interaction potential and diagonal in physical space for the bulk energy term—we develop a customized algorithm for solving the non-convex TR subproblem arising at each iteration of the IMEX-TR method. The solver computes the global minimizer of the subproblem with theoretical guarantees. The resulting implementation uses the fast Fourier transform (FFT) and achieves  $\mathcal{O}(N \log N)$  computational complexity per iteration.
- The numerical results show that the IMEX-TR method reliably converges to SP-IIs from a wide range of initializations and effectively avoids SDPs encountered by first-order schemes. Furthermore, we reveal a previously unreported SP-II, namely the FDDD pattern, in the LB model and determine its stable region within the newly constructed phase diagram.

The remainder of this article is organized as follows. Section 2 discretizes the LB energy functional via the Fourier pseudospectral method, obtaining the finite-dimensional optimization problem. Section 3 proposes the IMEX-TR method and provides a comprehensive convergence analysis to SP-IIs. This section also details the construction and theoretical analysis of the efficient global solver for the nonconvex TR subproblem. Section 4 presents numerical results that validate the theoretical properties of the proposed method. Finally, Section 5 provides a summary of the main findings.

**Notation:** In the rest of the content, let  $\|\mathbf{u}\|_2 = \sqrt{\mathbf{u}^\top \mathbf{u}}$  denote the  $\ell_2$  norm for vector  $\mathbf{u}$ . The operator (spectral) norm of a matrix  $\mathbf{H}$  is denoted by  $\|\mathbf{H}\| := \max_{\|\mathbf{u}\|_2=1} \|\mathbf{H}\mathbf{u}\|_2$ . For a third-order tensor  $\mathcal{T}$  (e.g., third-order derivative  $\nabla^3 E$ ), the operator norm is defined as  $\|\mathcal{T}\| := \max_{\|\mathbf{u}\|_2=\|\mathbf{v}\|_2=\|\mathbf{w}\|_2=1} |\mathcal{T}[\mathbf{u}, \mathbf{v}, \mathbf{w}]|$ , which represents the maximum absolute value of the tensor evaluated over all unit vectors [10].

## 2. Discretizing the LB model with Fourier pseudospectral method.

Here, we consider the periodic structures of the LB model. Thus, we adopt the Fourier pseudospectral method for spatial discretization. This approach naturally accommodates periodic boundary conditions and facilitates the enforcement of mass conservation.

Consider a periodic order parameter  $\psi(\mathbf{x})$  defined on  $\mathbf{x} \in \mathbb{T}^d := \mathbb{R}^d / \mathbf{A}\mathbb{Z}^d$ , where  $\mathbf{A} \in \mathbb{R}^{d \times d}$  represents the primitive Bravais lattice. The primitive reciprocal lattice  $\mathbf{B} \in \mathbb{R}^{d \times d}$  satisfies the dual relationship  $\mathbf{A}\mathbf{B}^\top = 2\pi\mathbf{I}$ .

The order parameter  $\psi(\mathbf{x})$  can be expanded as

$$\psi(\mathbf{x}) = \sum_{\mathbf{k} \in \mathbb{Z}^d} \hat{\psi}(\mathbf{k}) e^{i(\mathbf{B}\mathbf{k})^\top \mathbf{x}}, \quad \mathbf{x} \in \mathbb{T}^d,$$

where the Fourier coefficients

$$\hat{\psi}(\mathbf{k}) = \frac{1}{|\mathbb{T}^d|} \int_{\Omega} \psi(\mathbf{x}) e^{-i(\mathbf{B}\mathbf{k})^\top \mathbf{x}} d\mathbf{x}.$$

Define the discrete grid set as

$$\mathbb{T}_M^d = \{(\mathbf{x}_{1,i_1}, \dots, \mathbf{x}_{d,i_d}) = \mathbf{A}(i_1/M, \dots, i_d/M)^\top, i_j = 0, \dots, M-1, j = 1, \dots, d\},$$

where the number of elements in  $\mathbb{T}_M^d$  is  $N = M^d$ . Denote the grid periodic function space  $\mathcal{F}_M = \{f : \mathbb{T}_M^d \rightarrow \mathbb{R}, f \text{ is periodic}\}$ . For any periodic grid functions  $f, g \in \mathcal{F}_M$ ,

define the discrete  $\ell^2$ -inner product as

$$\langle f, g \rangle_N = \frac{1}{N} \sum_{\mathbf{x}_i \in \mathbb{T}_M^d} f(\mathbf{x}_i) \bar{g}(\mathbf{x}_i),$$

where  $\bar{g}(\mathbf{x}_i)$  is the conjugate of  $g(\mathbf{x}_i)$ .

The discrete reciprocal space is

$$\mathbb{K}_M^d = \{\mathbf{k} = (k_i)_{i=1}^d \in \mathbb{Z}^d : -M/2 \leq k_i < M/2\}.$$

For  $\mathbf{k}, \mathbf{h} \in \mathbb{Z}^d$ , we have the discrete orthogonality

$$\langle e^{i(\mathbf{B}\mathbf{k})^\top \mathbf{x}}, e^{i(\mathbf{B}\mathbf{h})^\top \mathbf{x}} \rangle_N = \begin{cases} 1, & \mathbf{k} = \mathbf{h} + M\mathbf{m}, \mathbf{m} \in \mathbb{Z}^d, \\ 0, & \text{otherwise.} \end{cases}$$

Then the discrete Fourier coefficients of  $\psi(\mathbf{x})$  in  $\Omega_M$  can be represented as

$$\hat{\psi}(\mathbf{k}) = \langle \psi(\mathbf{x}), e^{i(\mathbf{B}\mathbf{k})^\top \mathbf{x}} \rangle_N = \frac{1}{N} \sum_{\mathbf{x}_i \in \mathbb{T}_M^d} \psi(\mathbf{x}_i) e^{-i(\mathbf{B}\mathbf{k})^\top \mathbf{x}_i}, \quad \mathbf{k} \in \mathbb{K}_M^d.$$

Let  $\hat{\Psi} = (\psi_1, \dots, \psi_N) \in \mathbb{R}^N$ , where  $\psi_i = \psi(\mathbf{x}_i)$ ,  $1 \leq i \leq N$ . Denote  $\mathcal{F}_N \in \mathbb{C}^{N \times N}$  as the discrete Fourier transformation matrix, then we have the discrete order parameter  $\hat{\Psi} = \mathcal{F}_N \Psi$  in reciprocal space. The discretized energy function is

$$E(\hat{\Psi}) = G(\hat{\Psi}) + F(\hat{\Psi}),$$

where  $G$  and  $F$  are the discretized interaction and bulk energy

$$(2.1) \quad \begin{aligned} G(\hat{\Psi}) &= \frac{1}{2} \sum_{\mathbf{k}_1 + \mathbf{k}_2 = 0} [1 - \mathbf{k}^\top \mathbf{k}]^2 \hat{\Psi}(\mathbf{k}_1) \hat{\Psi}(\mathbf{k}_2), \\ F(\hat{\Psi}) &= \frac{\tau}{2} \sum_{\mathbf{k}_1 + \mathbf{k}_2 = 0} \hat{\Psi}(\mathbf{k}_1) \hat{\Psi}(\mathbf{k}_2) - \frac{\gamma}{3!} \sum_{\mathbf{k}_1 + \mathbf{k}_2 + \mathbf{k}_3 = 0} \hat{\Psi}(\mathbf{k}_1) \hat{\Psi}(\mathbf{k}_2) \hat{\Psi}(\mathbf{k}_3) \\ &\quad + \frac{1}{4!} \sum_{\mathbf{k}_1 + \mathbf{k}_2 + \mathbf{k}_3 + \mathbf{k}_4 = 0} \hat{\Psi}(\mathbf{k}_1) \hat{\Psi}(\mathbf{k}_2) \hat{\Psi}(\mathbf{k}_3) \hat{\Psi}(\mathbf{k}_4), \end{aligned}$$

and  $\mathbf{k}_i \in \mathbb{K}_M^d$ . The nonlinear terms  $F(\hat{\Psi})$  can be efficiently obtained by the FFT after being calculated in the  $d$ -dimensional physical space. Moreover, the mass conservation constraint is discretized as

$$\mathbf{e}_1^\top \hat{\Psi} = 0,$$

where  $\mathbf{e}_1 = (1, 0, \dots, 0)^\top \in \mathbb{R}^N$ . Therefore, we obtain the finite-dimensional minimization problem

$$(2.2) \quad \min_{\hat{\Psi} \in \mathbb{C}^N} E(\hat{\Psi}) = G(\hat{\Psi}) + F(\hat{\Psi}) \quad \text{s.t.} \quad \mathbf{e}_1^\top \hat{\Psi} = 0.$$

According to (2.1), we have

$$\begin{aligned} \nabla G(\hat{\Psi}) &= \mathbf{\Lambda} \hat{\Psi}, & \nabla F(\hat{\Psi}) &= \mathcal{F}_N \mathbf{\Gamma} \mathcal{F}_N^{-1} \hat{\Psi}, \\ \nabla^2 G(\hat{\Psi}) &= \mathbf{\Lambda}, & \nabla^2 F(\hat{\Psi}) &= \mathcal{F}_N \mathbf{\Gamma}' \mathcal{F}_N^{-1}, \end{aligned}$$

where  $\mathbf{\Lambda}$  is a diagonal matrix with nonnegative entries  $[1 - \mathbf{k}^\top \mathbf{k}]^2$  and  $\mathbf{\Gamma}, \mathbf{\Gamma}' \in \mathbb{R}^{N \times N}$  are also diagonal matrices that depend on  $\hat{\Psi}$ .

**3. Implicit-Explicit Trust Region Method.** This section considers solving the minimization problem (2.2). To transform the problem into an unconstrained optimization problem, we use the following property

$$\{\hat{\Psi} \in \mathbb{C}^N : \mathbf{e}_1^\top \hat{\Psi} = 0\} = \{\mathbf{P}^\top \mathbf{v} : \mathbf{v} \in \mathbb{C}^{N-1}\},$$

where  $\mathbf{P} = [\mathbf{0}, \mathbf{I}_{N-1}]$ . Based on this, we introduce an equivalent objective function

$$\bar{E}(\mathbf{v}) = E(\mathbf{P}^\top \mathbf{v}),$$

we then can equivalently express problem (2.2) as the following unconstrained optimization problem

$$(3.1) \quad \min_{\mathbf{v} \in \mathbb{C}^{N-1}} \bar{E}(\mathbf{v}).$$

**3.1. IMEX-TR Method and Convergence Analysis.** In this subsection, we present the TR method (see Algorithm 3.1) and prove that this algorithm converges to SP-IIIs of the problem (3.1). At each iteration  $j$ , we construct a quadratic model  $m_j(\mathbf{d})$  of the objective function around the current iterate  $\mathbf{v}_j$ ,

$$m_j(\mathbf{d}) = \bar{E}(\mathbf{v}_j) + \mathbf{g}_j^\top \mathbf{d} + \frac{1}{2} \mathbf{d}^\top \mathbf{H}_j \mathbf{d},$$

where  $\mathbf{g}_j = \nabla \bar{E}(\mathbf{v}_j)$  and  $\mathbf{H}_j = \nabla^2 \bar{E}(\mathbf{v}_j)$ . The step  $\mathbf{d}_j$  is obtained by solving the TR subproblem

$$(3.2) \quad \min_{\|\mathbf{d}\|_2 \leq r_j} m_j(\mathbf{d}),$$

where  $r_j$  is the trust region radius. The optimality conditions for the TR subproblem (3.2) are stated in the following theorem.

**THEOREM 3.1** ([12], Corollary 7.2.2). *A vector  $\mathbf{d}_*$  is a global minimizer of the subproblem (3.2) if and only if there exists a scalar  $\lambda_* \geq 0$  such that the following conditions are satisfied.*

$$(3.3) \quad \begin{cases} \mathbf{g}_j + (\mathbf{H}_j + \lambda_* \mathbf{I}) \mathbf{d}_* = 0, \\ \|\mathbf{d}_*\|_2 - r_j \leq 0, \\ \lambda_*(\|\mathbf{d}_*\|_2 - r_j) = 0, \\ \mathbf{H}_j + \lambda_* \mathbf{I} \succeq 0. \end{cases}$$

*If  $\mathbf{H}_j + \lambda_* \mathbf{I}$  is positive definite, then  $\mathbf{d}_*$  is the unique global minimizer of (3.2).*

Algorithm 3.1 summarizes the IMEX-TR method for solving the problem (3.1). Algorithm 3.2, the CONTRACT procedure, is designed to adjust the trust region radius. Algorithm 3.3 in the next subsection will present the customized solver for the TR subproblem (3.2).

**3.1.1. Convergence to Second-Order Stationary Points.** We first present two important properties of the gradient and Hessian of the energy functional  $\bar{E}(\mathbf{v})$  with  $\{\mathbf{v}_j\}$  and  $\{\mathbf{s}_j\}$  generated by Algorithm 3.1.

**THEOREM 3.2.** *Let  $\mathbf{s}_j$  be the global minimizer of the TR subproblem at the  $j$ -th iteration of Algorithm 3.1, and let sequence  $\{\mathbf{v}_j\}$  be generated by Algorithm 3.1. Then the gradient sequence  $\{\nabla \bar{E}(\mathbf{v}_j)\}$  is bounded and the function  $\nabla \bar{E}$  is Lipschitz continuous with a scalar Lipschitz constant  $g_{Lip} > 0$  in an open convex set containing the iterate sequence  $\{\mathbf{v}_j\}$  and  $\{\mathbf{v}_j + \mathbf{s}_j\}$ . Furthermore, the Hessian function  $\nabla^2 \bar{E}$  is Lipschitz continuous on a path defined by the sequence of  $\{\mathbf{v}_j\}$  and  $\{\mathbf{v}_j + \mathbf{s}_j\}$ .*

---

**Algorithm 3.1** IMEX-TR method for solving the problem (3.1)

---

**Require:** Initial guess  $\mathbf{v}_0$ , initial radius  $r_0$ , parameters  $\theta \in (0, 1)$ ,  $0 < \gamma_C < 1 < \gamma_E$ ,  $\gamma_\lambda > 1$ ,  $0 < \underline{\mu} \leq \bar{\mu}$ ,  $\mu_0 \geq \underline{\mu}$ ,  $0 < r_0 \leq \nu_0$ , tolerance  $\varepsilon > 0$ .

- 1: **for**  $j = 0, 1, \dots$  **do**
- 2:     Compute  $\mathbf{g}_j = \nabla \bar{E}(\mathbf{v}_j)$
- 3:     **if**  $\|\mathbf{g}_j\|_\infty < \varepsilon$ , **return**  $\mathbf{v}_j$ . **end if**
- 4:     Solve the TR subproblem (3.2) (see Algorithm 3.3), let  $\mathbf{s}_j$  and  $\lambda_j$  satisfy the optimality conditions (3.3), and  $\mathbf{s}_j$  be the global minimizer.
- 5:     **if**  $j > 0$  and  $\varrho_{j-1} < \theta$  **then**
- 6:          $\mu_j = \max\{\mu_{j-1}, \lambda_j / \|\mathbf{s}_j\|_2\}$
- 7:     **end if**
- 8:     Calculate  $\varrho_j = (\bar{E}(\mathbf{v}_j) - \bar{E}(\mathbf{v}_j + \mathbf{s}_j)) / \|\mathbf{s}_j\|_2^3$
- 9:     **if**  $\varrho_j \geq \theta$  and either  $\lambda_j \leq \mu_j \|\mathbf{s}_j\|_2$  or  $\|\mathbf{s}_j\|_2 = \nu_j$  **then**
- 10:          $\mathbf{v}_{j+1} = \mathbf{v}_j + \mathbf{s}_j$ ,  $\nu_{j+1} = \max\{\nu_j, \gamma_E \|\mathbf{s}_j\|_2\}$
- 11:          $r_{j+1} = \min\{\nu_{j+1}, \max\{r_j, \gamma_E \|\mathbf{s}_j\|_2\}\}$ ,  $\mu_{j+1} = \max\{\mu_j, \lambda_j / \|\mathbf{s}_j\|_2\}$
- 12:     **else if**  $\varrho_j < \theta$  **then**
- 13:          $\mathbf{v}_{j+1} = \mathbf{v}_j$ ,  $\nu_{j+1} = \nu_j$ ,  $r_{j+1} = \text{CONTRACT}(\mathbf{v}_j, r_j, \mu_j, \mathbf{s}_j, \lambda_j)$ .
- 14:     **else**
- 15:          $\mathbf{v}_{j+1} = \mathbf{v}_j$ ,  $\nu_{j+1} = \nu_j$ ,  $r_{j+1} = \min\{\nu_{j+1}, \lambda_j / \mu_j\}$ ,  $\mu_{j+1} = \mu_j$
- 16:     **end if**
- 17: **end for**

---

*Proof.* By the continuity and coercivity of  $\bar{E}$  and the decrease of  $\bar{E}(\mathbf{v}_j)$ , the sublevel set  $\mathcal{L} = \{\mathbf{v} \mid \bar{E}(\mathbf{v}) \leq \bar{E}(\mathbf{v}_0)\}$  is compact and  $\{\mathbf{v}_j\} \subset \mathcal{L}$ , hence the sequences  $\{\mathbf{v}_j\}$  and  $\{\nabla \bar{E}(\mathbf{v}_j)\}$  are bounded. As the trial step  $\mathbf{s}_j$  is bounded  $\|\mathbf{s}_j\|_2 \leq r_j$ , thus  $\{\mathbf{v}_j + \mathbf{s}_j\}$  is also bounded. By the boundedness of  $\{\mathbf{v}_j\}$  and  $\{\mathbf{v}_j + \mathbf{s}_j\}$ , there exists  $R > 0$  such that  $\|\mathbf{v}_j\|_2 \leq R$  and  $\|\mathbf{v}_j + \mathbf{s}_j\|_2 \leq R$  for all  $j$ . Let  $\mathcal{B} := \{\mathbf{v} \mid \|\mathbf{v}\|_2 < R + \delta\}$ , where  $\delta > 0$ , then  $\mathcal{B}$  is a bounded open convex set containing  $\{\mathbf{v}_j\}$  and  $\{\mathbf{v}_j + \mathbf{s}_j\}$ .

By the mean value inequality, for any  $\mathbf{u}, \mathbf{v} \in \mathcal{B}$ ,

$$\|\nabla \bar{E}(\mathbf{u}) - \nabla \bar{E}(\mathbf{v})\| \leq \sup_{\mathbf{w} \in \bar{\mathcal{B}}} \|\nabla^2 \bar{E}(\mathbf{w})\| \|\mathbf{u} - \mathbf{v}\|_2,$$

where  $\bar{\mathcal{B}}$  is the closure of  $\mathcal{B}$ . By the continuity of  $\nabla^2 \bar{E}$  and the compactness of  $\bar{\mathcal{B}}$ , we have  $\sup_{\mathbf{w} \in \bar{\mathcal{B}}} \|\nabla^2 \bar{E}(\mathbf{w})\| < \infty$ , with  $g_{\text{Lip}} := \sup_{\mathbf{w} \in \bar{\mathcal{B}}} \|\nabla^2 \bar{E}(\mathbf{w})\|$ , the Lipschitz continuity of  $\nabla \bar{E}$  on  $\mathcal{B}$  follows.

To prove the Lipschitz continuity of  $\nabla^2 \bar{E}$  on the path defined by the sequences  $\{\mathbf{v}_j\}$  and  $\{\mathbf{v}_j + \mathbf{s}_j\}$ , we only need to show that  $\nabla^2 \bar{E}$  is Lipschitz continuous on  $\bar{\mathcal{B}}$ . According to the mean value inequality, for any  $\mathbf{u}, \mathbf{v} \in \bar{\mathcal{B}}$ , we have

$$\|\nabla^2 \bar{E}(\mathbf{u}) - \nabla^2 \bar{E}(\mathbf{v})\| \leq \sup_{\mathbf{w} \in \bar{\mathcal{B}}} \|\nabla^3 \bar{E}(\mathbf{w})\| \|\mathbf{u} - \mathbf{v}\|_2.$$

As the third-order derivative  $\nabla^3 \bar{E}$  exists and is continuous, it follows that

$$\|\nabla^2 \bar{E}(\mathbf{u}) - \nabla^2 \bar{E}(\mathbf{v})\| \leq h_{\text{Lip}} \|\mathbf{u} - \mathbf{v}\|_2,$$

where  $h_{\text{Lip}} := \sup_{\mathbf{w} \in \bar{\mathcal{B}}} \|\nabla^3 \bar{E}(\mathbf{w})\| < \infty$ . This completes the proof.  $\square$

With the above preparations, we can establish the convergence of the outer loop to SP-IIs.

---

**Algorithm 3.2** CONTRACT procedure
 

---

```

1: procedure CONTRACT( $\mathbf{v}_j, r_j, \mu_j, \mathbf{s}_j, \lambda_j$ )
2: if  $\lambda_j < \underline{\mu} \|\mathbf{s}_j\|_2$  then
3:    $\hat{\lambda} = \lambda_j + (\underline{\mu} \|\mathbf{g}_j\|_2)^{1/2}$ 
4:    $\tilde{\lambda} = \hat{\lambda}$ , solve the linear system  $(\mathbf{H}_j + \tilde{\lambda} \mathbf{I})\mathbf{s} = -\mathbf{g}_j$  to get  $\mathbf{s}$ 
5:   if  $\tilde{\lambda} / \|\mathbf{s}\|_2 \leq \bar{\mu}$  then
6:     return  $r_{j+1} = \|\mathbf{s}\|_2$ 
7:   else
8:     Find  $\tilde{\lambda} \in (\lambda_j, \hat{\lambda})$  such that  $\underline{\mu} \leq \tilde{\lambda} / \|\mathbf{s}\|_2 \leq \bar{\mu}$ , where  $\mathbf{s}$  is the solution of the
     linear system  $(\mathbf{H}_j + \tilde{\lambda} \mathbf{I})\mathbf{s} = -\mathbf{g}_j$ 
9:     return  $r_{j+1} = \|\mathbf{s}\|_2$ 
10:  end if
11: else
12:    $\tilde{\lambda} = \gamma_\lambda \lambda_j$  and solve the linear system  $(\mathbf{H}_j + \tilde{\lambda} \mathbf{I})\mathbf{s} = -\mathbf{g}_j$  to get  $\mathbf{s}$ 
13:   if  $\|\mathbf{s}\|_2 \geq \gamma_C \|\mathbf{s}_j\|_2$  then
14:     return  $r_{j+1} = \|\mathbf{s}\|_2$ 
15:   else
16:     return  $r_{j+1} = \gamma_C \|\mathbf{s}\|_2$ 
17:   end if
18: end if
19: end procedure

```

---

**THEOREM 3.3.** *The sequence  $\{\mathbf{v}_j\}$  generated by Algorithm 3.1 has the following property*

$$\lim_{j \rightarrow \infty} \|\nabla \bar{E}(\mathbf{v}_j)\| = 0, \quad \liminf_{j \rightarrow \infty} \nabla^2 \bar{E}(\mathbf{v}_j) \succeq 0.$$

*Proof.* In combination with Theorem 3.2, the properties of the sequence  $\{\mathbf{v}_j\}$  follow directly from Theorem 3.14 and Theorem 3.26 of [15].  $\square$

**3.2. Efficient Global Solver for the Nonconvex TR Subproblem.** In this subsection, we propose an efficient IMEX algorithm to solve the nonconvex TR subproblem (3.2) and analyze the algorithm's ability to converge to the global minimizer of the subproblem.

At each iteration of the IMEX-TR, a core challenge lies in solving the nonconvex subproblem (3.2) globally and efficiently. For ease of analysis, we remove the subscript  $j$  and the constant term, and restate the subproblem (3.2) as

$$(3.4) \quad \min_{\|\mathbf{d}\|_2 \leq r} f(\mathbf{d}) = \mathbf{g}^\top \mathbf{d} + \frac{1}{2} \mathbf{d}^\top \mathbf{H} \mathbf{d}.$$

We exploit the structural properties of the Hessian for the LB model, which can be decomposed as

$$\mathbf{H} = \underbrace{\mathbf{P} \nabla^2 G(\mathbf{P}^\top \mathbf{v}) \mathbf{P}^\top}_{\mathbf{D}} + \underbrace{\mathbf{P} \nabla^2 F(\mathbf{P}^\top \mathbf{v}) \mathbf{P}^\top}_{\mathbf{T}} = \mathbf{D} + \mathbf{T}.$$

Here,  $\mathbf{D}$  is a positive semi-definite diagonal matrix in reciprocal space.

We develop an algorithm that embeds an adaptive implicit-explicit iteration within the TR loop. The implicit-explicit scheme for the subproblem is

$$(3.5) \quad (\mathbf{I} + \eta(\mathbf{D} + \lambda_{k+1}\mathbf{I}))\mathbf{d}_{k+1} = \mathbf{d}_k - \eta(\mathbf{g} + \mathbf{T}\mathbf{d}_k), \quad k = 0, 1, 2, \dots$$

where  $\eta > 0$  is a step size, and  $\lambda_{k+1} \geq 0$  is a Lagrange multiplier adjusted to ensure  $\|\mathbf{d}_{k+1}\| \leq r_j$ . In this scheme, the diagonal part  $\mathbf{D}$  is treated implicitly while the dense part  $\mathbf{T}$  is treated explicitly, enabling efficient FFT-based computation while maintaining stability.

By letting  $\mathbf{L}_{k+1} = \mathbf{D} + \lambda_{k+1}\mathbf{I}$ ,  $\bar{\mathbf{g}}_k = \mathbf{g} + \mathbf{T}\mathbf{d}_k$ , and substituting these into (3.5), then it can be rewritten as

$$(3.6) \quad \underbrace{(\mathbf{I} + \eta\mathbf{L}_{k+1})}_{\text{Diagonal matrix}} \mathbf{d}_{k+1} = \mathbf{d}_k - \eta\bar{\mathbf{g}}_k.$$

The features of scheme (3.6) are

- The matrix  $\mathbf{I} + \eta\mathbf{L}_{k+1}$  is a diagonal matrix in reciprocal space, thus the update process only involves element-wise operations on the matrix, resulting in low computational complexity.
- The coefficient matrix  $\mathbf{I} + \eta\mathbf{L}_{k+1}$  is always positive definite, which guarantees the existence and uniqueness of the solution to the linear system, ensuring the numerical stability of the scheme.
- By adjusting the value of  $\lambda_{k+1}$ , the norm of the solution can be limited within a certain range to ensure that the solution is within the feasible domain of the subproblem.

*Remark 3.4.* In order to exploit the diagonal structure of  $\mathbf{T}$  in physical space, the product  $\mathbf{T}\mathbf{d}$  is efficiently computed by performing point-wise multiplication in physical space followed by the FFT. This approach ensures an overall computational complexity of  $\mathcal{O}(N \log N)$  per iteration, avoiding the  $\mathcal{O}(N^2)$  cost associated with direct matrix-vector multiplication in reciprocal space.

We first show that the solution of (3.6) satisfies  $\|\mathbf{d}\|_2 \leq r$  by adaptively adjusting the value of  $\lambda_{k+1}$ , which ensures the solution of the adaptive implicit-explicit iteration is a feasible solution to problem (3.4).

Since  $\mathbf{I} + \eta\mathbf{L}_{k+1}$  is a diagonal matrix and positive definite, we get

$$\mathbf{d}_{k+1} = (\mathbf{I} + \eta\mathbf{L}_{k+1})^{-1}\mathbf{b}_k = \begin{pmatrix} [\mathbf{b}_k]_1 / (1 + \eta(\mathbf{D}_{1,1} + \lambda_{k+1})) \\ \vdots \\ [\mathbf{b}_k]_{N-1} / (1 + \eta(\mathbf{D}_{N-1,N-1} + \lambda_{k+1})) \end{pmatrix},$$

where  $[\mathbf{b}_k]_i$  denotes the  $i$ -th component of  $\mathbf{b}_k = \mathbf{d}_k - \eta\bar{\mathbf{g}}_k$  and  $D_{i,i}$  is the  $i$ -th diagonal element of the diagonal matrix  $\mathbf{D}$ , thus

$$\phi_k(\lambda_{k+1}) = \|\mathbf{d}_{k+1}\|_2^2 = \sum_{i=1}^{N-1} \left( \frac{[\mathbf{b}_k]_i}{(1 + \eta(\mathbf{D}_{i,i} + \lambda_{k+1}))} \right)^2,$$

it is easy to see that  $\phi_k(\lambda)$  is a continuously differentiable and monotonically decreasing function with respect to  $\lambda$ , then there must exist  $0 \leq \lambda_{\min} \leq \lambda_{\max} < \infty$ , such that for any  $\lambda_{k+1} \in [\lambda_{\min}, \lambda_{\max}]$ , we have  $\phi_k(\lambda_{k+1}) \leq r^2$ . We set the value of  $\lambda_{k+1}$  as

$$(3.7) \quad \lambda_{k+1} = \begin{cases} 0, & \text{if } \phi_k(0) \leq r^2, \\ \lambda', & \text{if } \phi_k(0) > r^2, \end{cases}$$

where  $\lambda'$  satisfying  $\phi_k(\lambda') = r^2$  is computed via Newton's method

$$\lambda_{\iota+1} = \lambda_{\iota} - (\phi_k(\lambda_{\iota}) - r^2) / \phi'_k(\lambda_{\iota}), \iota = 0, 1, 2, \dots,$$

with  $\lambda_0 = 0$ . The complete adaptive implicit-explicit iteration for solving the TR subproblem (3.4) is summarized in Algorithm 3.3.

---

**Algorithm 3.3** Adaptive implicit-explicit iteration

---

**Input:** : Step size  $\eta > 0$ , trust region radius  $r > 0$ , gradient  $\mathbf{g}$ , decompose Hessian as  $\mathbf{H} = \mathbf{D} + \mathbf{T}$ , initial value  $\mathbf{d}_0 = -r\mathbf{g}/\|\mathbf{g}\|_2$ , tolerance  $\varepsilon_{\text{sub}}$ .

**Output:**  $\mathbf{d}_{k+1}$ .

```

for  $k = 0, 1, \dots$  do
   $\lambda_{k+1} = 0$ .
  while  $\phi_k(\lambda_{k+1}) > r^2$  do
    Find  $\lambda_{k+1}$  satisfies  $\phi_k(\lambda_{k+1}) = r^2$  by Newton's method
     $\lambda_{k+1} \leftarrow \lambda_{k+1} - (\phi_k(\lambda_{k+1}) - r^2) / \phi'_k(\lambda_{k+1})$ 
  end while
   $\mathbf{d}_{k+1} = (\mathbf{I} + \eta(\mathbf{D} + \lambda_{k+1}\mathbf{I}))^{-1}(\mathbf{d}_k - \eta(\mathbf{g} + \mathbf{T}\mathbf{d}_k))$ 
  if  $\|\mathbf{g} + (\mathbf{H} + \lambda_{k+1}\mathbf{I})\mathbf{d}_{k+1}\|_2 < \varepsilon_{\text{sub}}$  then
    return  $\mathbf{d}_{k+1}$ .
  end if
end for

```

---

By Algorithm 3.3 and the update rule (3.7), we have the following corollary.

**COROLLARY 3.5.** *The sequence  $\{(\lambda_k, \mathbf{d}_k)\}$  generated by Algorithm 3.3 has the following properties,*

$$\lambda_k \geq 0, \quad \|\mathbf{d}_k\|_2 \leq r, \quad \lambda_k(\|\mathbf{d}_k\|_2 - r) = 0.$$

By the above Corollary 3.5, we need only focus on the remaining two conditions in the optimality conditions (3.3). In the following, we first focus on the condition  $\mathbf{g} + (\mathbf{H} + \lambda^*\mathbf{I})\mathbf{d}^* = 0$ , and then the condition  $\mathbf{H} + \lambda^*\mathbf{I} \succeq 0$ .

**3.2.1. Global Convergence of the IMEX solver for the TR subproblem.**

We analyze the properties of the sequence  $\{\mathbf{d}_k\}$  generated by Algorithm 3.3 for solving the nonconvex subproblem.

Let  $\beta^2 = \lambda \geq 0$  and define the Lagrangian function associated with the TR subproblem (3.4) as

$$(3.8) \quad L(\mathbf{d}, \beta) = f(\mathbf{d}) + \frac{\beta^2}{2}(\|\mathbf{d}\|_2^2 - r^2).$$

We first present the following Lemma 3.6 to describe the decreasing property of function values of  $L$ , which plays a crucial role in proving the convergence for the scheme (3.6).

**LEMMA 3.6.** *For any  $a > 0$ , if step size  $\eta$  satisfies the inequality*

$$\eta^{-1} \geq \|\mathbf{T}\| + 2a,$$

*then we get the descent property for the function values of  $f$  in (3.4) and  $L$  in (3.8),*

$$\begin{aligned} f(\mathbf{d}_k) - f(\mathbf{d}_{k+1}) &\geq a\|\mathbf{d}_{k+1} - \mathbf{d}_k\|_2^2, \\ L(\mathbf{d}_k, \beta_k) - L(\mathbf{d}_{k+1}, \beta_{k+1}) &\geq a\|\mathbf{d}_{k+1} - \mathbf{d}_k\|_2^2. \end{aligned}$$

*Proof.* We define an auxiliary function and show that the update rule (3.6) is equivalent to minimizing this auxiliary function, *i.e.*,

$$(3.9) \quad \mathbf{d}_{k+1} = \arg \min_{\mathbf{d}} \{f_k(\mathbf{d})\},$$

where the objective function is defined as

$$f_k(\mathbf{d}) = \frac{1}{2} \mathbf{d}^\top \mathbf{L}_{k+1} \mathbf{d} + (\mathbf{g} + \frac{1}{2} \mathbf{T} \mathbf{d}_k)^\top \mathbf{d}_k + \bar{\mathbf{g}}_k^\top (\mathbf{d} - \mathbf{d}_k) + \frac{1}{2\eta} \|\mathbf{d} - \mathbf{d}_k\|_2^2,$$

By the optimality of  $\mathbf{d}_{k+1}$  in (3.9), we have

$$\begin{aligned} & f(\mathbf{d}_k) + \frac{\beta_{k+1}^2}{2} \|\mathbf{d}_k\|_2^2 = f_k(\mathbf{d}_k) \geq f_k(\mathbf{d}_{k+1}) \\ &= \frac{1}{2} (\mathbf{d}_{k+1})^\top \mathbf{L}_{k+1} (\mathbf{d}_{k+1}) + (\mathbf{g} + \frac{1}{2} \mathbf{T} \mathbf{d}_k)^\top (\mathbf{d}_{k+1}) + (\bar{\mathbf{g}}_k)^\top (\mathbf{d}_{k+1} - \mathbf{d}_k) + \frac{1}{2\eta} \|\mathbf{d}_{k+1} - \mathbf{d}_k\|_2^2 \\ &= \frac{1}{2} (\mathbf{d}_{k+1})^\top (\mathbf{D} \mathbf{d}_{k+1}) + (\mathbf{g})^\top (\mathbf{d}_{k+1}) + (\mathbf{T} \mathbf{d}_{k+1})^\top (\mathbf{d}_{k+1} - \mathbf{d}_k) + \frac{1}{2\eta} \|\mathbf{d}_{k+1} - \mathbf{d}_k\|_2^2 \\ &\quad - (\mathbf{T} (\mathbf{d}_{k+1} - \mathbf{d}_k))^\top (\mathbf{d}_{k+1} - \mathbf{d}_k) + \frac{1}{2} (\mathbf{T} \mathbf{d}_k)^\top (\mathbf{d}_k) + \frac{\beta_{k+1}^2}{2} \|\mathbf{d}_{k+1}\|_2^2 \\ &= f(\mathbf{d}_{k+1}) + \frac{\beta_{k+1}^2}{2} \|\mathbf{d}_{k+1}\|_2^2 + \frac{1}{2\eta} \|\mathbf{d}_{k+1} - \mathbf{d}_k\|_2^2 + \frac{1}{2} (\mathbf{T} \mathbf{d}_{k+1})^\top (\mathbf{d}_{k+1}) \\ &\quad - (\mathbf{T} (\mathbf{d}_{k+1} - \mathbf{d}_k))^\top (\mathbf{d}_{k+1} - \mathbf{d}_k) + \frac{1}{2} (\mathbf{T} \mathbf{d}_k)^\top (\mathbf{d}_k) - (\mathbf{T} \mathbf{d}_{k+1})^\top (\mathbf{d}_k) \\ &= f(\mathbf{d}_{k+1}) + \frac{\beta_{k+1}^2}{2} \|\mathbf{d}_{k+1}\|_2^2 + \frac{1}{2\eta} \|\mathbf{d}_{k+1} - \mathbf{d}_k\|_2^2 - \frac{1}{2} (\mathbf{T} (\mathbf{d}_{k+1} - \mathbf{d}_k))^\top (\mathbf{d}_{k+1} - \mathbf{d}_k) \\ &= f(\mathbf{d}_{k+1}) + \frac{\beta_{k+1}^2}{2} \|\mathbf{d}_{k+1}\|_2^2 + \frac{1}{2} (\mathbf{d}_{k+1} - \mathbf{d}_k)^\top (\frac{1}{\eta} \mathbf{I} - \mathbf{T}) (\mathbf{d}_{k+1} - \mathbf{d}_k). \end{aligned}$$

Since  $\|\mathbf{d}_k\|_2^2 \leq r^2$ , it follows that

$$f(\mathbf{d}_k) + \frac{\beta_{k+1}^2}{2} \|\mathbf{d}_k\|_2^2 \leq f(\mathbf{d}_k) + \frac{\beta_{k+1}^2}{2} r^2.$$

By combining the above inequality with Corollary 3.5, we have

$$f(\mathbf{d}_k) + \frac{\beta_{k+1}^2}{2} r^2 \geq f(\mathbf{d}_{k+1}) + \frac{\beta_{k+1}^2}{2} r^2 + \frac{1}{2} \langle \mathbf{d}_{k+1} - \mathbf{d}_k, (\frac{1}{\eta} \mathbf{I} - \mathbf{T}) (\mathbf{d}_{k+1} - \mathbf{d}_k) \rangle.$$

Thus, when  $1/\eta \geq \|\mathbf{T}\| + 2a$ , it reads

$$f(\mathbf{d}_k) - f(\mathbf{d}_{k+1}) \geq a \|\mathbf{d}_{k+1} - \mathbf{d}_k\|_2^2,$$

and

$$\begin{aligned} & L(\mathbf{d}_k, \beta_k) - L(\mathbf{d}_{k+1}, \beta_{k+1}) \\ &= f(\mathbf{d}_k) + \frac{\beta_k^2}{2} (\|\mathbf{d}_k\|_2^2 - r^2) - \left( f(\mathbf{d}_{k+1}) + \frac{\beta_{k+1}^2}{2} (\|\mathbf{d}_{k+1}\|_2^2 - r^2) \right) \\ &= f(\mathbf{d}_k) - f(\mathbf{d}_{k+1}) \\ &\geq a \|\mathbf{d}_{k+1} - \mathbf{d}_k\|_2^2. \end{aligned}$$

The second equality above is derived from Corollary 3.5.  $\square$

Next, we show that the norm of the gradient is bounded, which is also important to our convergence theorem.

LEMMA 3.7. *If the step size  $\eta$  satisfies*

$$(3.10) \quad 0 < \eta_{\min} \leq \eta \leq \frac{1}{\|\mathbf{T}\| + 2a},$$

then there must exist  $b > 0$ , such that

$$(3.11) \quad \left\| \begin{pmatrix} \nabla_{\mathbf{d}} L(\mathbf{d}_{k+1}, \beta_{k+1}) \\ \nabla_{\beta} L(\mathbf{d}_{k+1}, \beta_{k+1}) \end{pmatrix} \right\|_2 \leq b \|\mathbf{d}_{k+1} - \mathbf{d}_k\|_2.$$

*Proof.*

$$\begin{aligned} & \left\| \begin{pmatrix} \nabla_{\mathbf{d}} L(\mathbf{d}_{k+1}, \beta_{k+1}) \\ \nabla_{\beta} L(\mathbf{d}_{k+1}, \beta_{k+1}) \end{pmatrix} \right\|_2 = \left\| \begin{pmatrix} \nabla f(\mathbf{d}_{k+1}) + \beta_{k+1}^2 \mathbf{d}_{k+1} \\ \beta_{k+1} (\|\mathbf{d}_{k+1}\|_2^2 - r^2) \end{pmatrix} \right\|_2 \\ &= \left\| \begin{pmatrix} \nabla f(\mathbf{d}_{k+1}) + \beta_{k+1}^2 \mathbf{d}_{k+1} \\ 0 \end{pmatrix} \right\|_2 \\ &= \|\mathbf{g} + \mathbf{T}\mathbf{d}_k + \mathbf{D}\mathbf{d}_{k+1} + \beta_{k+1}^2 \mathbf{d}_{k+1} + \mathbf{T}(\mathbf{d}_{k+1} - \mathbf{d}_k)\|_2 \\ &= \|\mathbf{g} - (\mathbf{d}_{k+1} - \mathbf{d}_k)/\eta + \mathbf{T}(\mathbf{d}_{k+1} - \mathbf{d}_k)\|_2 \\ &\leq (1/\eta + \|\mathbf{T}\|) \|\mathbf{d}_{k+1} - \mathbf{d}_k\|_2 \\ &\leq (1/\eta_{\min} + \|\mathbf{T}\|) \|\mathbf{d}_{k+1} - \mathbf{d}_k\|_2. \end{aligned}$$

The second equality above follows from Corollary 3.5 and  $\beta_{k+1}^2 = \lambda_{k+1}$ , (3.5) has been used for the fourth equality. Let  $b = 1/\eta_{\min} + \|\mathbf{T}\|$  finishes the proof.  $\square$

Using the KL property and the techniques of Lemma 2.6 from [2], we prove that the sequence  $\{\mathbf{d}_k\}$  is a Cauchy sequence.

DEFINITION 3.8 (KL Property[5]). *Let  $L : \mathbb{C}^N \rightarrow (-\infty, +\infty]$  be a proper and lower semi-continuous function. For each  $\mathbf{z}_* \in \text{dom } \nabla L$ , there exist  $\kappa > 0$ , a neighborhood  $U$  of  $\mathbf{z}_*$ , and a concave continuous function  $\varphi : [0, \kappa) \rightarrow \mathbb{R}_+$ , such that*

$$\varphi(0) = 0, \quad \varphi \in \mathbb{C}^1(0, \kappa), \quad \varphi'(s) > 0 \text{ for all } s \in (0, \kappa), \text{ and}$$

$$\varphi'(L(\mathbf{z}) - L(\mathbf{z}_*)) \text{dist}(0, \nabla L(\mathbf{z})) \geq 1,$$

for all  $\mathbf{z} \in U \cap \{\mathbf{z} : L(\mathbf{z}_*) < L(\mathbf{z}) < L(\mathbf{z}_*) + \kappa\}$ , then  $L(\mathbf{z})$  is said to satisfy the KL property at point  $\mathbf{z}_*$ . If  $L(\mathbf{z})$  satisfies the KL property at every point  $\mathbf{z}$ , then  $L(\mathbf{z})$  is called a KL function.

THEOREM 3.9. *Let the sequence  $\{\mathbf{z}_k\} = \{(\mathbf{d}_k, \beta_k)\} = \{(\mathbf{d}_k, \sqrt{\lambda_k})\}$  be generated by the IMEX subproblem solver in Algorithm 3.1. If the step condition (3.10) is satisfied, then we have that*

$$\sum_{k=1}^{\infty} \|\mathbf{d}_k - \mathbf{d}_{k+1}\|_2 < \infty,$$

which means  $\{\mathbf{d}_k\}$  is a Cauchy sequence and that  $\{\mathbf{d}_k\}$  converges to  $\mathbf{d}_*$  as  $k \rightarrow \infty$ .

*Proof.* As  $\{\mathbf{z}_k\}$  is bounded, there must exist an accumulation point of  $\{\mathbf{z}_k\}$ , let it be  $\mathbf{z}_* = (\mathbf{d}_*, \beta_*)$ , and there exists a subsequence  $\{\mathbf{z}_{k_l}\}$  of  $\{\mathbf{z}_k\}$  converging to  $\mathbf{z}_*$  as  $l \rightarrow \infty$ . Due to the boundedness from below of  $L$  and the monotonicity of  $\{L(\mathbf{z}_k)\}$ ,

the continuous property of  $L$  implies that  $\{L(\mathbf{z}_k)\}$  converges to  $L(\mathbf{z}_*)$  as  $k \rightarrow \infty$  with  $L(\mathbf{z}_*) < L(\mathbf{z}_k)$ ,  $k \in \mathbb{N}$ . In particular,  $L$  satisfies the KL property [5], and thus

$$L(\mathbf{z}_*) < L(\mathbf{z}_k) < L(\mathbf{z}_*) + \kappa \text{ for large } k \in \mathbb{N} \text{ and small } \kappa > 0.$$

Taking the latter into account, we define a sequence  $\{b_k\}$  by

$$b_k := \|\mathbf{z}_k - \mathbf{z}_*\|_2 + 2(a^{-1}(L(\mathbf{z}_k) - L(\mathbf{z}_*)))^{\frac{1}{2}} + ba^{-1}\varphi(L(\mathbf{z}_k) - L(\mathbf{z}_*))$$

and deduce from the continuity of  $\varphi$  that the origin  $0 \in \mathbb{R}$  is an accumulation point of  $\{b_k\}$ . Thus there exists  $k_0 := k_{l_0}$  such that the inequalities

$$(3.12) \quad \|\mathbf{z}_{k_0} - \mathbf{z}_*\|_2 + 2(a^{-1}(L(\mathbf{z}_{k_0}) - L(\mathbf{z}_*)))^{\frac{1}{2}} + ba^{-1}\varphi(L(\mathbf{z}_{k_0}) - L(\mathbf{z}_*)) < \epsilon,$$

$$L(\mathbf{z}_*) < L(\mathbf{z}_{k_0}) < L(\mathbf{z}_*) + \kappa$$

are satisfied and yield in turn the inclusions

$$\mathbf{z}_{k_0} \in B(\mathbf{z}_*, \epsilon) \cap [L(\mathbf{z}_*) < L < L(\mathbf{z}_*) + \kappa] \subset U \cap [L(\mathbf{z}_*) < L < L(\mathbf{z}_*) + \kappa],$$

hence  $\mathbf{d}_{k_0} \in B(\mathbf{d}_*, \epsilon)$ .

Moreover, we claim that if  $L(\mathbf{z}_k) < L(\mathbf{z}_*) + \kappa$  and  $\mathbf{d}_k \in B(\mathbf{d}_*, \epsilon)$ , then

$$(3.13) \quad 2\|\mathbf{d}_{k+1} - \mathbf{d}_k\|_2 \leq \|\mathbf{d}_k - \mathbf{d}_{k-1}\|_2 + \frac{b}{a}[\varphi(L(\mathbf{z}_k) - L(\mathbf{z}_*)) - \varphi(L(\mathbf{z}_{k+1}) - L(\mathbf{z}_*))].$$

By Lemma 3.6, we have the inequality

$$(3.14) \quad L(\mathbf{z}_k) - L(\mathbf{z}_{k+1}) \geq a\|\mathbf{d}_{k+1} - \mathbf{d}_k\|_2^2,$$

hence

$$0 \leq L(\mathbf{z}_{k_0+1}) - L(\mathbf{z}_*) \leq L(\mathbf{z}_{k_0}) - L(\mathbf{z}_*) < \kappa,$$

which implies therefore the inequality

$$\varphi(L(\mathbf{z}_{k_0}) - L(\mathbf{z}_*)) - \varphi(L(\mathbf{z}_{k_0+1}) - L(\mathbf{z}_*)) \geq \varphi'(L(\mathbf{z}_{k_0}) - L(\mathbf{z}_*))(L(\mathbf{z}_{k_0}) - L(\mathbf{z}_{k_0+1}))$$

by the concavity of  $\varphi$ . Combining (3.14) and

$$\varphi'(L(\mathbf{z}_{k_0}) - L(\mathbf{z}_*)) \geq \frac{1}{\nabla L(\mathbf{d}_{k_0}, \beta_{k_0})} \geq \frac{1}{b\|\mathbf{d}_{k_0} - \mathbf{d}_{k_0-1}\|_2},$$

we have

$$\frac{b}{a}[\varphi(L(\mathbf{z}_{k_0}) - L(\mathbf{z}_*)) - \varphi(L(\mathbf{z}_{k_0+1}) - L(\mathbf{z}_*))] \geq \frac{\|\mathbf{d}_{k_0+1} - \mathbf{d}_{k_0}\|_2^2}{\|\mathbf{d}_{k_0} - \mathbf{d}_{k_0-1}\|_2}.$$

By  $2\sqrt{\alpha\beta} \leq \alpha + \beta$ , we get (3.13) with  $k = k_0$ , *i.e.*,

$$2\|\mathbf{d}_{k_0+1} - \mathbf{d}_{k_0}\|_2 \leq \|\mathbf{d}_{k_0} - \mathbf{d}_{k_0-1}\|_2 + \frac{b}{a}[\varphi(L(\mathbf{z}_{k_0}) - L(\mathbf{z}_*)) - \varphi(L(\mathbf{z}_{k_0+1}) - L(\mathbf{z}_*))].$$

As we have

$$(3.15) \quad \|\mathbf{d}_{k_0+1} - \mathbf{d}_{k_0}\|_2 \leq \sqrt{\frac{L(\mathbf{z}_{k_0}) - L(\mathbf{z}_{k_0+1})}{a}} \leq \sqrt{\frac{L(\mathbf{z}_{k_0}) - L(\mathbf{z}_*)}{a}}$$

by (3.14), hence

$$\|\mathbf{d}_{k_0+1} - \mathbf{d}_*\|_2 \leq \|\mathbf{d}_{k_0} - \mathbf{d}_*\|_2 + \|\mathbf{d}_{k_0+1} - \mathbf{d}_{k_0}\|_2 \leq \|\mathbf{d}_{k_0} - \mathbf{d}_*\|_2 + \sqrt{\frac{L(\mathbf{z}_{k_0}) - L(\mathbf{z}_*)}{a}} < \epsilon,$$

then  $\mathbf{d}_{k_0+1} \in B(\mathbf{d}_*, \epsilon)$ , we get (3.13) with  $k = k_0 + 1$ , *i.e.*,

$$2\|\mathbf{d}_{k_0+2} - \mathbf{d}_{k_0+1}\|_2 \leq \|\mathbf{d}_{k_0+1} - \mathbf{d}_{k_0}\|_2 + \frac{b}{a}[\varphi(L(\mathbf{z}_{k_0+1}) - L(\mathbf{z}_*)) - \varphi(L(\mathbf{z}_{k_0+2}) - L(\mathbf{z}_*))].$$

Next, for  $l = 1, 2, \dots$ , we prove  $\mathbf{d}_{k_0+l} \in B(\mathbf{d}_*, \epsilon)$  and

$$(3.16) \quad \begin{aligned} & \sum_{i=1}^l \|\mathbf{d}_{k_0+i+1} - \mathbf{d}_{k_0+i}\|_2 + \|\mathbf{d}_{k_0+l+1} - \mathbf{d}_{k_0+l}\|_2 \\ & \leq \|\mathbf{d}_{k_0+1} - \mathbf{d}_{k_0}\|_2 + \frac{b}{a}[\varphi(L(\mathbf{z}_{k_0+1}) - L(\mathbf{z}_*)) - \varphi(L(\mathbf{z}_{k_0+l+1}) - L(\mathbf{z}_*))] \end{aligned}$$

by induction on  $l$ . Suppose  $\mathbf{d}_{k_0+l} \in B(\mathbf{d}_*, \epsilon)$  and (3.16) hold for some  $l \geq 1$ , using the triangle inequality and (3.16) we have

$$\begin{aligned} \|\mathbf{d}_* - \mathbf{d}_{k_0+l+1}\|_2 & \leq \|\mathbf{d}_* - \mathbf{d}_{k_0}\|_2 + \|\mathbf{d}_{k_0} - \mathbf{d}_{k_0+1}\|_2 + \sum_{i=1}^l \|\mathbf{d}_{k_0+i+1} - \mathbf{d}_{k_0+i}\|_2 \\ & \leq \|\mathbf{d}_* - \mathbf{d}_{k_0}\|_2 + 2\|\mathbf{d}_{k_0} - \mathbf{d}_{k_0+1}\|_2 \\ & \quad + \frac{b}{a}[\varphi(L(\mathbf{z}_{k_0+1}) - L(\mathbf{z}_*)) - \varphi(L(\mathbf{z}_{k_0+l+1}) - L(\mathbf{z}_*))] \\ & \leq \|\mathbf{d}_* - \mathbf{d}_{k_0}\|_2 + 2\|\mathbf{d}_{k_0} - \mathbf{d}_{k_0+1}\|_2 + \frac{b}{a}[\varphi(L(\mathbf{z}_{k_0}) - L(\mathbf{z}_*))]. \end{aligned}$$

Using the above inequality, (3.15) and (3.12) we conclude that  $\mathbf{d}_{k_0+l+1} \in B(\mathbf{d}_*, \epsilon)$ . Hence, (3.13) holds with  $k = k_0 + l + 1$ , *i.e.*,

$$\begin{aligned} 2\|\mathbf{d}_{k_0+l+2} - \mathbf{d}_{k_0+l+1}\|_2 & \leq \|\mathbf{d}_{k_0+l+1} - \mathbf{d}_{k_0+l}\|_2 + \\ & \quad \frac{b}{a}[\varphi(L(\mathbf{z}_{k_0+l+1}) - L(\mathbf{z}_*)) - \varphi(L(\mathbf{z}_{k_0+l+2}) - L(\mathbf{z}_*))]. \end{aligned}$$

Adding the above inequality with (3.16), yields (3.16) with  $l + 1$ , which completes the induction proof.

Direct use of (3.16) shows that

$$\sum_{i=k_0+1}^{k_0+l} \|\mathbf{d}_{i+1} - \mathbf{d}_i\|_2 \leq \|\mathbf{d}_{k_0+1} - \mathbf{d}_{k_0}\|_2 + \frac{b}{a}(\varphi(L(\mathbf{z}_{k_0+1}) - L(\mathbf{z}_*))),$$

therefore,

$$\sum_{i=1}^{\infty} \|\mathbf{d}_{i+1} - \mathbf{d}_i\|_2 < +\infty$$

which implies that the sequence  $\{\mathbf{d}_k\}$  is a Cauchy sequence, which therefore converges to  $\mathbf{d}_*$  since it is an accumulation point of  $\{\mathbf{d}_k\}$ .  $\square$

Thus, we can prove that any limit point  $\{(\mathbf{d}_*, \lambda_*)\}$  of sequence  $\{(\mathbf{d}_k, \lambda_k)\}$  is a KKT point.

THEOREM 3.10. *When step size condition (3.10) is satisfied, every limit point  $\{(\mathbf{d}_*, \lambda_*)\}$  of the sequence  $\{(\mathbf{d}_k, \lambda_k)\}$  is a KKT point of problem (3.4).*

*Proof.* As  $\{\lambda_k\}$  is a bounded sequence, by the Bolzano-Weierstrass theorem, there exists a subsequence  $\{\lambda_{k_l}\}$  such that  $\lambda_{k_l} \rightarrow \lambda_*$  as  $l \rightarrow \infty$ . By Theorem 3.9 we know that  $\mathbf{d}_k$  converges to  $\mathbf{d}_*$ , thus  $\lim_{k \rightarrow \infty} \|\mathbf{d}_{k+1} - \mathbf{d}_k\|_2 = 0$ . Taking the limits along the convergent subsequence on both sides of (3.11) yields

$$\lim_{j \rightarrow \infty} \|\mathbf{g} + \mathbf{D}\mathbf{d}_{k_l+1} + \mathbf{T}\mathbf{d}_{k_l} + \lambda_{k_l+1}\mathbf{d}_{k_l+1}\|_2 = 0 \implies \mathbf{g} + \mathbf{D}\mathbf{d}_* + \mathbf{T}\mathbf{d}_* + \lambda_*\mathbf{d}_* = 0,$$

combining with Corollary 3.5, we conclude that  $(\mathbf{d}_*, \lambda_*)$  is a KKT point of problem (3.4).  $\square$

Finally, we establish the global convergence of Algorithm 3.3. Denote by  $\sigma_1 \leq \sigma_2 \leq \dots \leq \sigma_{N-1}$  the eigenvalues of  $\mathbf{H}$  in (3.4). If  $\sigma_1 \geq 0$ , then subproblem (3.4) is a convex problem, and thus the first-order convergence (Theorem 3.10) naturally guarantees the global convergence of the iteration. Below, we assume  $\sigma_1 < 0$  and choose  $\boldsymbol{\xi}$  to be the unit-norm eigenvector of the matrix  $\mathbf{H}$  corresponding to the smallest eigenvalue  $\sigma_1$  (i.e.,  $\|\boldsymbol{\xi}\|_2 = 1$ ). We define  $w^{(1)} := \boldsymbol{\xi}^\top \mathbf{w}$ , for any  $\mathbf{w} \in \mathbb{R}^{N-1}$ . The proof of global convergence relies on the following proposition.

PROPOSITION 3.11 (Proposition 2.2 [9]). *Let  $g^{(1)} \neq 0$ . The global minimizer  $\mathbf{d}_*$  of problem (3.4) is the unique stationary point satisfying the condition  $d_*^{(1)}g^{(1)} \leq 0$ .*

Building upon the above proposition, we further prove that the limit point  $\mathbf{d}_*$  from Theorem 3.10 is the global minimizer of the subproblem (3.4).

THEOREM 3.12. *If  $g^{(1)} \neq 0$  and the initial point is chosen as  $\mathbf{d}_0 = -r\mathbf{g}/\|\mathbf{g}\|_2$ , then there exists an  $\eta_{\max} > 0$  such that for any step size  $\eta \in (\eta_{\min}, \eta_{\max}]$ ,  $\mathbf{d}_*$  is the global minimizer of the subproblem (3.4).*

*Proof.* Theorem 3.10 establishes that  $\mathbf{d}_k \rightarrow \mathbf{d}_*$  and that  $\mathbf{d}_*$  is a KKT point of (3.4). By Proposition 3.11, we only need to prove that

$$(3.17) \quad d_*^{(1)}g^{(1)} \leq 0.$$

We now use induction to establish that

$$(3.18) \quad d_k^{(1)}g^{(1)} \leq 0 \quad \text{for all } k \geq 0,$$

and thus taking the limit yields (3.17). By the choice of the initial point, we have

$$d_0^{(1)}g^{(1)} = -r(g^{(1)})^2 \leq 0.$$

Next, assuming  $d_k^{(1)}g^{(1)} \leq 0$ , we show  $d_{k+1}^{(1)}g^{(1)} \leq 0$ . We rewrite the iteration (3.5) as

$$(3.19) \quad \begin{aligned} & [\mathbf{I} + \eta(\mathbf{D} + \lambda_{k+1}\mathbf{I})]\mathbf{d}_{k+1} = \mathbf{d}_k - \eta(\mathbf{T}\mathbf{d}_k + \mathbf{g}) = \mathbf{d}_k - \eta((\mathbf{H} - \mathbf{D})\mathbf{d}_k + \mathbf{g}) \\ & = (\mathbf{I} + \eta\mathbf{D})\mathbf{d}_k - \eta(\mathbf{H}\mathbf{d}_k + \mathbf{g}) = (\mathbf{I} + \eta\mathbf{D})\mathbf{d}_k - \eta\nabla f(\mathbf{d}_k) \\ & = (\mathbf{I} + \eta(\mathbf{D} + \lambda_{k+1}\mathbf{I}))\mathbf{d}_k - \eta(\lambda_{k+1}\mathbf{d}_k + \nabla f(\mathbf{d}_k)). \end{aligned}$$

Then

$$(3.20) \quad \mathbf{d}_{k+1} = \mathbf{d}_k - \eta(\mathbf{I} + \eta(\mathbf{D} + \lambda_{k+1}\mathbf{I}))^{-1}(\lambda_{k+1}\mathbf{d}_k + \nabla f(\mathbf{d}_k)).$$

Multiplying both sides of equation (3.19) on the left by  $\boldsymbol{\xi}$  yields

$$(1 + \eta\lambda_{k+1})d_{k+1}^{(1)} + \eta\langle \boldsymbol{\xi}, \mathbf{D}(\mathbf{d}_{k+1} - \mathbf{d}_k) \rangle = (1 - \eta\sigma_1)d_k^{(1)} - \eta g^{(1)}.$$

Multiplying both sides of the equation by  $g^{(1)}$  yields

$$(1 + \eta\lambda_{k+1})d_{k+1}^{(1)}g^{(1)} = (1 - \eta\sigma_1)d_k^{(1)}g^{(1)} - \eta \left( (g^{(1)})^2 + \langle \boldsymbol{\xi}, \mathbf{D}(\mathbf{d}_{k+1} - \mathbf{d}_k) \rangle g^{(1)} \right).$$

Since  $d_k^{(1)}g^{(1)} \leq 0$ , sufficient conditions for  $d_{k+1}^{(1)}g^{(1)} \leq 0$  are

$$(3.21a) \quad 1 - \eta\sigma_1 \geq 0 \iff \eta \geq \frac{1}{\sigma_1};$$

$$(3.21b) \quad (g^{(1)})^2 + \langle \boldsymbol{\xi}, \mathbf{D}(\mathbf{d}_{k+1} - \mathbf{d}_k) \rangle g^{(1)} \geq 0.$$

With  $\mathbf{M}_k = \mathbf{D}[\mathbf{I} + \eta(\mathbf{D} + \lambda_{k+1}\mathbf{I})]^{-1}$ , we analyze the conditions under which (3.21b) holds. From the iteration (3.20), we have

$$(3.22) \quad \begin{aligned} \|\mathbf{D}(\mathbf{d}_{k+1} - \mathbf{d}_k)\|_2 &= \|\eta\mathbf{M}_k(\lambda_{k+1}\mathbf{d}_k + \nabla f(\mathbf{d}_k))\|_2 \\ &\leq \eta\|\mathbf{M}_k\| \|\lambda_{k+1}\mathbf{d}_k + \nabla f(\mathbf{d}_k)\|_2 \\ &= \frac{\eta\|\mathbf{D}\| \|\lambda_{k+1}\mathbf{d}_k + \nabla f(\mathbf{d}_k)\|_2}{1 + \eta(\|\mathbf{D}\| + \lambda_{k+1})} \\ &\leq \frac{\eta\|\mathbf{D}\|(\lambda_{\max}\|\mathbf{d}_k\|_2 + \|\nabla f(\mathbf{d}_k)\|_2)}{1 + \eta\|\mathbf{D}\|}. \end{aligned}$$

There exists  $\bar{\eta} > 0$  such that, for all  $\eta \leq \bar{\eta}$ , we have

$$(3.23) \quad \frac{\eta\|\mathbf{D}\|(\lambda_{\max}\|\mathbf{d}_k\|_2 + \|\nabla f(\mathbf{d}_k)\|_2)}{1 + \eta\|\mathbf{D}\|} < \frac{|g^{(1)}|}{2}, \quad \text{for all } k \geq 0.$$

Combining (3.22), (3.23) and  $\|\boldsymbol{\xi}\|_2 = 1$ , we have

$$\begin{aligned} (g^{(1)})^2 + \boldsymbol{\xi}^\top(\mathbf{D}(\mathbf{d}_{k+1} - \mathbf{d}_k))g^{(1)} &\geq (g^{(1)})^2 - \|\boldsymbol{\xi}\|_2 \|\mathbf{D}(\mathbf{d}_{k+1} - \mathbf{d}_k)\|_2 |g^{(1)}| \\ &> (g^{(1)})^2 - \frac{|g^{(1)}|^2}{2} = \frac{(g^{(1)})^2}{2} > 0. \end{aligned}$$

Thus, combining the step size condition (3.10) and (3.21a), if the step size  $\eta$  satisfies the following condition

$$\max \left\{ \frac{1}{\sigma_1}, \eta_{\min} \right\} = \eta_{\min} \leq \eta \leq \eta_{\max} := \min \left\{ \frac{1}{\|\mathbf{T}\| + 2a}, \bar{\eta} \right\},$$

it is guaranteed that  $d_{k+1}^{(1)}g^{(1)} \leq 0$ . Thus, by induction, (3.18) holds. Let  $k \rightarrow \infty$  in (3.18) and using Proposition 3.11, we conclude that  $\mathbf{d}_*$  must be a global minimizer of problem (3.4).  $\square$

**4. Numerical Experiments.** This section presents a comprehensive numerical evaluation of the proposed IMEX-TR method. To systematically compare the proposed method with several representative first-order schemes, including gradient flow methods and a Bregman proximal gradient algorithm, we demonstrate that IMEX-TR consistently converges to SP-IIs, whereas conventional methods often stagnate at

unstable SP-Is. Furthermore, we show that IMEX-TR exhibits robustness to initialization and is capable of escaping saddle points to explore complex energy landscapes, leading to the discovery of a previously unreported stable phase cubic FDDD in the LB model.

Parameters used in Algorithm 3.1 are set to standard values in TR literature to balance convergence speed and numerical stability,  $\gamma_C = 0.5$ ,  $\gamma_E = 2$ ,  $\gamma_\lambda = 1.5$ ,  $\theta = 10^{-4}$ ,  $\underline{\mu} = 1$ ,  $\bar{\mu} = 10^5$ ,  $\mu_0 = 1$ ,  $r_0 = 1$ ,  $\nu_0 = 5$  and  $\varepsilon = 10^{-10}$ . In Algorithm 3.3, the step size  $\eta = 0.1$  is chosen empirically to ensure efficient inner-loop convergence with a tolerance  $\varepsilon_{\text{sub}} = 10^{-13}$ .

**4.1. Convergence.** In this subsection, we compare the IMEX-TR method with representative methods, including the adaptive accelerated Bregman proximal gradient (AA-BPG) [18], and several gradient flow methods, including the semi-implicit scheme (SIS), first-order stabilized semi-implicit scheme (SSIS1), second-order stabilized semi-implicit scheme (SSIS2) [33], the invariant energy quadratization (IEQ) [38], the scalar auxiliary variable (SAV) [32], and exponential time differencing (ETD) methods [16].<sup>1</sup> All algorithms start from the same initial condition to demonstrate that the IMEX-TR method, by effectively using Hessian information, converges to SP-IIs, while other methods may converge to SP-Is.

We illustrate the performance of IMEX-TR through three different examples. Table 4.1 summarizes the model parameters  $(\tau, \gamma)$ , computational domains, and initial configurations employed in the three numerical experiments. The initial ordered configurations—specifically, three-dimensional lamellar (LAM) and hexagonal (HEX) phases—are constructed via Fourier series expansion of the form [19]

$$\psi(\mathbf{x}) = \sum_{\mathbf{k} \in \Xi} \hat{\psi}(\mathbf{k}) e^{i(\mathbf{B}\mathbf{k})^\top \mathbf{x}},$$

where the reciprocal lattice point sets  $\Xi$ , Fourier coefficients  $\hat{\psi}(\mathbf{k})$ , and reciprocal lattices  $\mathbf{B}$  are detailed in Table 4.2.

Table 4.1: Model parameters, computational domains, and initial configurations for three numerical examples.

Example	Parameters $(\tau, \gamma)$	Domain	Initial Phase
1	$(-0.35, 0.7)$	$[0, 2\sqrt{2}\pi]^3$	LAM
2	$(-0.001, 0.4)$	$[0, 2\sqrt{2}\pi]^3$	LAM
3	$(-0.28, 0.32)$	$[0, 2\sqrt{6}\pi]^3$	HEX

Figure 4.1 presents the converged SPs and their corresponding energy values. In Examples 1 and 2, conventional first-order schemes fail to escape the initial energy basins and stagnate at unstable stationary points. Specifically, in Example 1, first-order methods remain trapped in the LAM state, while in Example 2, they converge to a disordered state (*i.e.*,  $\phi(\mathbf{x}) \approx 0$ ). In contrast, the IMEX-TR method successfully converges to SP-IIs, HEX and body-centered cubic (BCC) phases, both exhibiting lower free energies. In Example 3, all methods reach the SP-II state HEX; however, the IMEX-TR method escapes the HEX basin and discovers a cubic FDDD pattern

<sup>1</sup>Since the results of SIS, SSIS1, and IEQ are similar to those of other methods except IMEX-TR, the corresponding results are not reported.

Table 4.2: Initial reciprocal lattice point sets  $\Xi$ , nonzero Fourier coefficients  $\hat{\psi}(\mathbf{k})$ , and reciprocal lattice matrices  $\mathbf{B}$  for the LAM and HEX phases.

Phase	$\Xi$	$\hat{\psi}(\mathbf{k})$	$\mathbf{B}$
LAM	$\{(1, 0, 0), (-1, 0, 0)\}$	0.3	$\frac{1}{\sqrt{2}}\mathbf{I}$
HEX	$\{(0, 1, -1), (0, -1, 1), (1, 0, -1), (-1, 0, 1), (1, -1, 0), (-1, 1, 0)\}$	0.3	$\frac{1}{\sqrt{6}}\mathbf{I}$

that achieves an energy of  $E = -8.05 \times 10^{-2}$ , which is markedly lower than the HEX phase ( $E = -8.02 \times 10^{-2}$ ). The cubic FDDD pattern has been reported in the phase diagram of AB-type diblock copolymers [37]; however, its presence in the LB model has not been previously documented.

To further verify the stability of these stationary points, we perform an eigenvalue analysis of the Hessian matrix. Figure 4.2 illustrates the evolution of the four smallest eigenvalues throughout the iterative process. For the first-order methods in Examples 1 and 2, the persistence of significant negative eigenvalues confirms that the states reached are SDPs. Conversely, the IMEX-TR method converges to a point where the Hessian eigenvalues are non-negative, which satisfies the SP-II condition.

In summary, the numerical results demonstrating convergence to SP-IIs and the discovery of the cubic FDDD phase highlight the IMEX-TR method's distinctive capability for identifying (meta-)stable states, while existing first-order gradient approaches may fail to capture.

$(\tau, \gamma)$	AA-BPG	SSIS2	SAV	ETD	IMEX-TR
(-0.35, 0.7)	 E=-1.94e-02	 E=-1.94e-02	 E=-1.94e-02	 E=-1.94e-02	 <b>E=-1.33e-01</b>
(-0.001, 0.4)	 E=2.68e-20	 E=4.02e-20	 E=4.02e-20	 E=4.02e-20	 <b>E=-1.10e-03</b>
(-0.28, 0.32)	 E=-8.02e-02	 E=-8.02e-02	 E=-8.02e-02	 E=-8.02e-02	 <b>E=-8.05e-02</b>

Fig. 4.1: Final physical phases and energy. IMEX-TR identifies the (meta-)stable HEX, BCC, and cubic FDDD phases across the three examples, consistently achieving lower energy states compared to standard first-order schemes.

**4.2. Robustness to initial conditions.** We further evaluate the robustness of IMEX-TR by activating it at distinct stages along the trajectory of first-order methods. As Figure 4.3 illustrates, IMEX-TR launches on three representative states: (i)

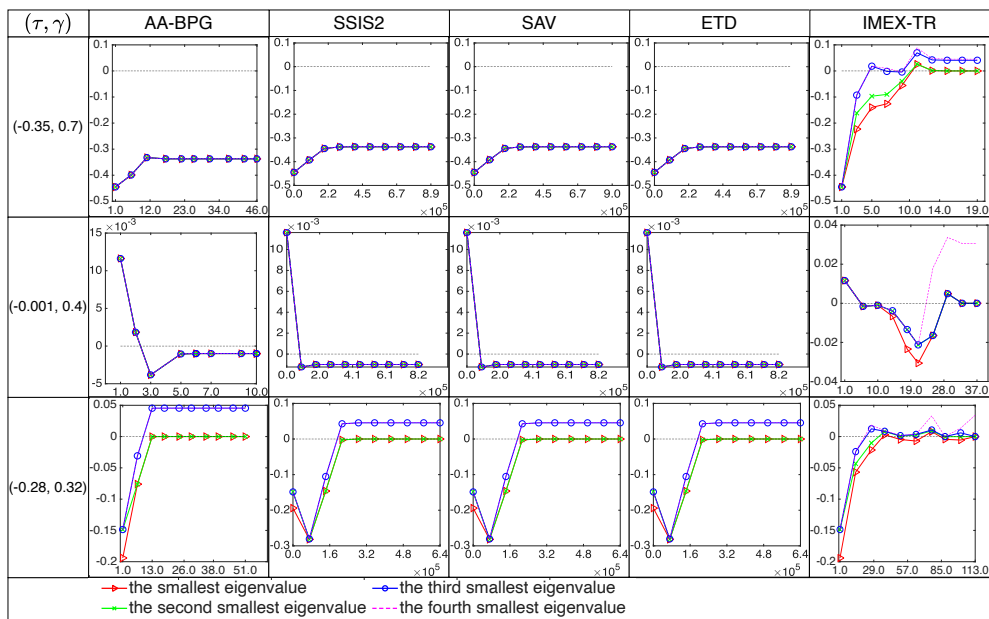


Fig. 4.2: Evolution of the four smallest eigenvalues of the Hessian matrix. The dashed line indicates the zero threshold. IMEX-TR consistently reaches the SP-II region (non-negative eigenvalues), whereas first-order methods often stagnate at SDPs with negative curvature.

the initial configuration, (ii) an intermediate state, and (iii) the converged SDP stage attained by first-order solvers. The behavior of IMEX-TR remains similar regardless of the specific first-order method used.

These results show that IMEX-TR consistently converges to an SP-II, a fundamental advantage arising from its use of Hessian information to capture the curvature of the energy landscape. This capability allows the algorithm to identify and exploit descent directions associated with negative curvature, thereby enabling it to divert the optimization trajectory away from SP-Is during the early stages or to escape them after stagnation. Consequently, the IMEX-TR reliably avoids SP-I and locates SP-II, *i.e.*, the physical (meta-)stable phase, regardless of whether it is deployed from the beginning or as a post-processing step for other solvers.

**4.3. Construction of new phase diagram.** The phase diagram of the LB model has been well documented to contain stable ordered phases such as LAM, HEX, BCC, double gyroid (DG), face-centered cubic spheres, A15, and  $\sigma$  phases [6, 26]. Our simulation in Section 4.1 demonstrates that the cubic FDDD pattern is indeed an SP-II according to the IMEX-TR method. There is a stable region of the discovered cubic FDDD pattern in the phase diagram of AB-type diblock copolymers [37]. However, its thermodynamic stability in the LB model remains uncertain. Motivated by this finding, we conducted an extensive search across the  $(\tau, \gamma)$  parameter space to investigate whether a stable region for the cubic FDDD pattern exists within the LB model. As presented in Figure 4.4, our results confirm the existence of a stable region for the cubic FDDD pattern. Moreover, the identified stable region of the cubic FDDD

phase does not affect the stable regions of the face-centered cubic spheres, A15, and  $\sigma$  phases [26]. This finding not only provides a more complete picture of the LB phase diagram but also demonstrates the capability of IMEX-TR to explore complex energy landscapes and uncover new stable structures.

**5. Conclusion.** In this work, we propose the IMEX-TR method for computing SP-IIs of a broad class of Landau-type energy functionals, which correspond to the (meta-)stable states of the physical system. Using the periodic phases of the LB model as a benchmark, we discretized the energy by the Fourier pseudospectral method and addressed the key algorithmic challenge, *i.e.*, solving the nonconvex TR subproblem with global optimality guarantees. By splitting the Hessian into two components that are diagonal in reciprocal space and in physical space, respectively, we developed an efficient solver that attains the global minimizer of each subproblem, thereby enabling the overall IMEX-TR iteration to provably converge to SP-IIs. Extensive numerical experiments on the LB model validate both the theoretical properties and the practical advantages of IMEX-TR, including robust convergence from diverse initializations and effective avoidance of SP-Is encountered by first-order gradient schemes. Furthermore, we identified the stable region of the cubic FDDD phase, which, to the best of our knowledge has not been reported in existing LB phase diagrams. Finally, although our analysis and experiments focused on the LB model, the IMEX-TR framework and the accompanying convergence theory are applicable to other Landau-type models of similar type and various spatial discretization schemes.

#### REFERENCES

- [1] N. Agarwal, Z. Allen-Zhu, B. Bullins, E. Hazan, and T. Ma. Finding approximate local minima faster than gradient descent. In *STOC'17—Proceedings of the 49th Annual ACM SIGACT Symposium on Theory of Computing*, pages 1195–1199. ACM, New York, 2017.
- [2] H. Attouch, J. Bolte, and B. F. Svaiter. Convergence of descent methods for semi-algebraic and tame problems: proximal algorithms, forward-backward splitting, and regularized Gauss-Seidel methods. *Math. Program.*, 137(1-2):91–129, 2013.
- [3] C. Bao, C. Chen, and K. Jiang. An adaptive block Bregman proximal gradient method for computing stationary states of multicomponent phase-field crystal model. *CSIAM Trans. Appl. Math.*, 3(1):133–171, 2022.
- [4] C. Bao, C. Chen, K. Jiang, and L. Qiu. Convergence analysis for Bregman iterations in minimizing a class of Landau free energy functionals. *SIAM J. Numer. Anal.*, 62(1):476–499, 2024.
- [5] J. Bolte, S. Sabach, and M. Teboulle. Proximal alternating linearized minimization for nonconvex and nonsmooth problems. *Math. Program.*, 146(1-2):459–494, 2014.
- [6] S. A. Brazovskii. Phase transition of an isotropic system to a nonuniform state. *Sov. Phys. JETP*, 41:85, 1975.
- [7] S. A. Brazovskii. Phase transition of an isotropic system to a nonuniform state. In *30 Years Of The Landau Institute—Selected Papers*, pages 109–113. World Scientific, 1996.
- [8] M. E. Caplan and C. J. Horowitz. Colloquium: Astromaterial science and nuclear pasta. *Rev. Modern Phys.*, 89:041002, 2017.
- [9] Y. Carmon and J. C. Duchi. First-order methods for nonconvex quadratic minimization. *SIAM Rev.*, 62(2):395–436, 2020. Revised reprint of “Gradient descent finds the cubic-regularized nonconvex Newton step” [4000224].
- [10] C. Cartis, N. I. M. Gould, and P. L. Toint. Sharp worst-case evaluation complexity bounds for arbitrary-order nonconvex optimization with inexpensive constraints. *SIAM J. Optim.*, 30(1):513–541, 2020.
- [11] L. Q. Chen and J. Shen. Applications of semi-implicit fourier-spectral method to phase field equations. *Computer Physics Communications*, 108(2-3):147–158, 1998.
- [12] A. R. Conn, N. I. M. Gould, and P. L. Toint. *Trust-region methods*. MPS/SIAM Series on Optimization. Society for Industrial and Applied Mathematics (SIAM), Philadelphia, PA; Mathematical Programming Society (MPS), Philadelphia, PA, 2000.
- [13] G. Cui and K. Jiang. Spring pair method of finding saddle points using the minimum energy

- path as a compass. *Phys. Rev. E*, 110(6):Paper No. 064123, 11, 2024.
- [14] G. Cui, K. Jiang, and T. Zhou. An efficient saddle search method for ordered phase transitions involving translational invariance. *Computer Physics Communications*, 306:109381, 2025.
- [15] F. E. Curtis, D. P. Robinson, and M. Samadi. A trust region algorithm with a worst-case iteration complexity of  $\mathcal{O}(\epsilon^{-3/2})$  for nonconvex optimization. *Math. Program.*, 162(1-2):1–32, 2017.
- [16] Z. Fu and J. Yang. Energy-decreasing exponential time differencing Runge-Kutta methods for phase-field models. *J. Comput. Phys.*, 454:Paper No. 110943, 11, 2022.
- [17] V. L. Ginzburg and L. D. Landau. On the theory of superconductivity. In *On superconductivity and superfluidity: a scientific autobiography*, pages 113–137. Springer, 2009.
- [18] K. Jiang, W. Si, C. Chen, and C. Bao. Efficient numerical methods for computing the stationary states of phase field crystal models. *SIAM J. Sci. Comput.*, 42(6):B1350–B1377, 2020.
- [19] K. Jiang, C. Wang, Y. Huang, and P. Zhang. Discovery of new metastable patterns in diblock copolymers. *Commun. Comput. Phys.*, 14(2):443–460, 2013.
- [20] C. Jin, R. Ge, P. Netrapalli, S. M. Kakade, and M. I. Jordan. How to escape saddle points efficiently. In *International conference on machine learning*, pages 1724–1732. PMLR, 2017.
- [21] L. D. Landau. The theory of phase transitions. *Nature*, 138(3498):840–841, 1936.
- [22] L. D. Landau and E. M. Lifshitz. *Statistical physics*, volume 5. Pergamon Press, 1958.
- [23] J. D. Lee, M. Simchowitz, M. I. Jordan, and B. Recht. Gradient descent only converges to minimizers. In *Conference on learning theory*, pages 1246–1257. PMLR, 2016.
- [24] L. Lin, X. Cheng, W. E, A.-C. Shi, and P. Zhang. A numerical method for the study of nucleation of ordered phases. *J. Comput. Phys.*, 229(5):1797–1809, 2010.
- [25] C. Liu and J. Shen. A phase field model for the mixture of two incompressible fluids and its approximation by a Fourier-spectral method. *Phys. D*, 179(3-4):211–228, 2003.
- [26] D. McClenagan. Landau theory of complex ordered phases. Master’s thesis, McMaster University, 2019.
- [27] Y. Nesterov and B. T. Polyak. Cubic regularization of Newton method and its global performance. *Math. Program.*, 108(1):177–205, 2006.
- [28] J. W. Neuberger. *Sobolev gradients and differential equations*, volume 1670 of *Lecture Notes in Mathematics*. Springer-Verlag, Berlin, second edition, 2010.
- [29] M. Nouiehed and M. Razaviyayn. A trust region method for finding second-order stationarity in linearly constrained nonconvex optimization. *SIAM J. Optim.*, 30(3):2501–2529, 2020.
- [30] C. W. Royer, M. O’Neill, and S. J. Wright. A Newton-CG algorithm with complexity guarantees for smooth unconstrained optimization. *Math. Program.*, 180(1-2):451–488, 2020.
- [31] S. Savitz, M. Babadi, and R. Lifshitz. Multiple-scale structures: from faraday waves to soft-matter quasicrystals. *IUCrJ*, 5(3):247–268, 2018.
- [32] J. Shen, J. Xu, and J. Yang. A new class of efficient and robust energy stable schemes for gradient flows. *SIAM Rev.*, 61(3):474–506, 2019.
- [33] J. Shen and X. Yang. Numerical approximations of Allen-Cahn and Cahn-Hilliard equations. *Discrete Contin. Dyn. Syst.*, 28(4):1669–1691, 2010.
- [34] S. Sial, J. Neuberger, T. Lookman, and A. Saxena. Energy minimization using Sobolev gradients: application to phase separation and ordering. *J. Comput. Phys.*, 189(1):88–97, 2003.
- [35] J. Swift and P. C. Hohenberg. Hydrodynamic fluctuations at the convective instability. *Phys. Rev. A*, 15(1):319–328, 1977.
- [36] S. M. Wise, C. Wang, and J. S. Lowengrub. An energy-stable and convergent finite-difference scheme for the phase field crystal equation. *SIAM J. Numer. Anal.*, 47(3):2269–2288, 2009.
- [37] K. Yamada, M. Nonomura, and T. Ohta. Fddd structure in AB-type diblock copolymers. *Journal of Physics: Condensed Matter*, 18(32):L421, 2006.
- [38] X. Yang. Linear, first and second-order, unconditionally energy stable numerical schemes for the phase field model of homopolymer blends. *J. Comput. Phys.*, 327:294–316, 2016.
- [39] P. Zhang and X. Zhang. An efficient numerical method of Landau-Brazovskii model. *J. Comput. Phys.*, 227(11):5859–5870, 2008.

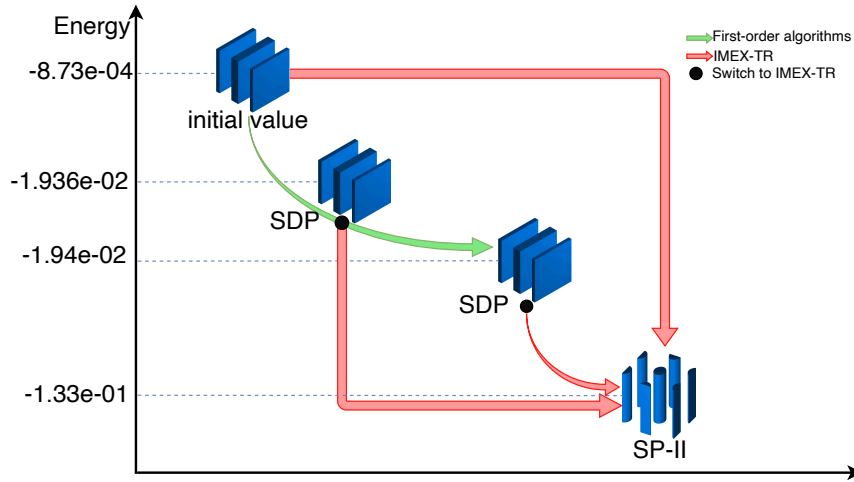


Fig. 4.3: Trajectories of IMEX-TR activated at different stages of first-order methods. Whether started from the initial point, an intermediate state, or the converged saddle point, IMEX-TR consistently converges to the same (meta-)stable SP-II (HEX phase), demonstrating its efficacy in exploiting negative curvature directions to escape unstable stationary points.

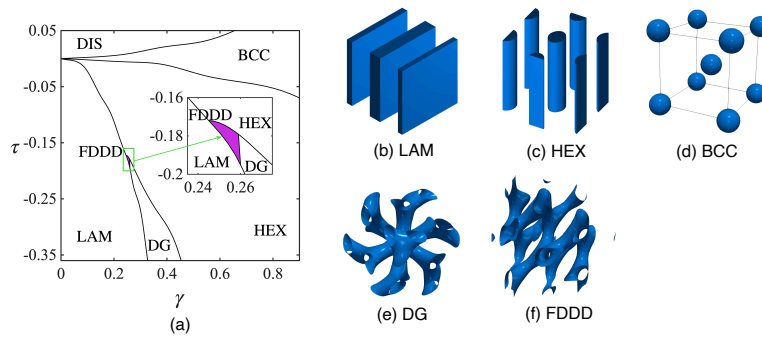


Fig. 4.4: (a) Phase diagram of the LB model. The purple shaded area corresponds to the stable region of the FDDD phase. (b)-(f) illustrate the SP-II phases: LAM, HEX, BCC, DG, and FDDD.